Synergistic Effects in Aqueous Solutions of Mixed Wormlike Micelles and Hydrophobically Modified Polymers

Isabelle Couillet,* Trevor Hughes, and Geoffrey Maitland

Schlumberger Cambridge Research, High Cross, Madingley Road Cambridge, CB3 OEL, U.K.

Françoise Candau

Institut Charles Sadron, UPR 22 du CNRS, 6 rue Boussingault, F-67083 Strasbourg Cedex, France.

Received January 25, 2005; Revised Manuscript Received March 15, 2005

ABSTRACT: The linear and nonlinear rheological properties of a hydrophobically modified guar (hm-HPG) and a surfactant forming wormlike micelles, the erucyl bis(hydroxyethyl)methylammonium chloride, have been investigated in 0.4 M KCl aqueous solution. The comparison between the zero-shear viscosity behaviors of the nonmodified guar and the hm-HPG shows a decrease of the intermolecular associations upon increasing the temperature. Significant synergistic effects were observed between the modified polymer and the wormlike micelles in a range of concentrations extending from 0.1 to 1 wt % and for temperatures up to 60 °C. The optimal synergy for the zero-shear viscosity is obtained for mixtures with an overall concentration ≈ 0.35 wt % and a surfactant/polymer ratio equal to 1/4 (w/w). The terminal time of the stress relaxation, the zero-shear viscosity as well as the viscosity at a shear rate of 100 s^{-1} and the lifetime of the associations show a maximum at this composition. The experimental observations suggest the formation of very efficient cross-links between the wormlike micelles and the polymer chains.

Introduction

Water-soluble hydrophobically modified polysaccharide derivatives are commonly used as thickening and rheology-control agents in aqueous systems.[1−4] The specific rheological behavior of such polymeric systems arises from their ability to give rise to weak intra- and intermolecular interactions between the hydrophobic groups distributed along the polymer chains. In the semidilute entangled regime, which is the domain of interest for most industrial applications, the hydrophobic moieties build up a transitory tridimensional network interpenetrated with the entanglement network. This microstructure leads to a slowing down of the polymer diffusion and to an increase in the zero-shear viscosity when compared to the analogues without the hydrophobes.[5−9] A model based on a sticky reptation process of the polymer chains has been proposed to describe the viscoelastic properties of these systems.[10−11]

Aqueous solutions of guar and its derivatives are the most widely used hydraulic fracturing fluids for the hydrocarbon recovery from subterranean formations, mainly for economical reasons.[5,12,13] The main functions of hydraulic fracturing fluids are to initiate and propagate the fracture and to transport the proppant along the length of the fracture. However, polymer-based fracturing fluids present the disadvantage of at least partially clogging the pore space in the fracture, so that the fracture is not optimally cleaned up. Recently, a new class of fracturing fluids based on viscoelastic surfactants forming wormlike micelles has been developed.[14−16] During backflow, as the surfactant gel comes into contact with the produced hydrocarbons, the wormlike micelles break down, forming spherical micelles, resulting in a low viscosity fluid which is more easily removed from the pore space in the propped fracture. Cationic surfactants with long mono-unsaturated tails (C_{22}) have been shown to be efficient fracturing fluids.[17] In particular, aqueous solutions of erucylbis(hydroxyethyl)-methylammonium chloride (EHAC) exhibit appropriate viscosities up to high temperatures (80 °C).[18−20]

In view of the above, it seemed appealing to investigate the rheological behavior of mixed surfactant/polymer aqueous solutions and particularly mixed viscoelastic surfactant/hydrophobically modified polymer (HMWSP) aqueous solutions. Many studies on the interactions between surfactants and HMWSP have been reported.[21−24] They generally concern systems in which the surfactant concentration is close to the critical micellar concentration (cmc). Under these conditions, one observes an enhancement of the zero-shear viscosity due either to the formation of additional mixed plurifunctional aggregates or to an increase in the lifetime of the preexisting cross-links resulting from surfactant binding.[13,25−34] To our knowledge, only one study has been reported which investigates the rheological properties of mixtures of wormlike micelles and hydrophobically modified polymer; specifically, this study focused on mixtures of cetyltrimethylammonium bromide (CTAB) and hm-hydroxyethylcellulose (with C_{16} hydrophobic substitution) in the presence of KBr.[35]

In the first part of this paper, we report a comparison of the flow behavior of hydroxypropyl guar (HPG) and its hydrophobically modified analogue (hm-HPG). A rheological study on these polymers under salt-free conditions and at T = 25 °C has been previously reported.[5] In the present study, we have investigated the same systems in the presence of salt and at various temperatures. These conditions are of primary importance for applications, mainly in oil recovery processes. Concerning the effect of temperature, only a limited number of studies have been performed, with contradictory conclusions. Some authors claim that an increase in temperature favors hydrophobic interactions[36−38] while the reverse is suggested by others.[39−40] In fact,

* Corresponding author. E-mail: couillet@cambridge.oilfield.slb.com.

10.1021/ma0501592 CCC: $30.25
Published on Web 05/07/2005

the effect of temperature might be strongly dependent on the nature of the polymer and of the quality of the diluent.

In the second part of the paper, we report a study on the synergistic effects occurring in the viscoelastic behavior of mixtures of 0.4 M KCl aqueous solutions containing EHAC surfactant and hm-HPG polymer in a concentration domain from 0.01 to 2.5 wt % and in a temperature range from 25 to 80 °C. The micellar growth and the viscoelastic properties of EHAC surfactant were described in a recent paper.[20]

Experimental Section

Materials. The HPG and hm-HPG polymers investigated here have been supplied by Fratelli Lamberti spa (Albizzate-Italy). The HPG sample is hydroxypropyl guar containing an average of one hydrophilic substituent (hydroxypropyl group) per monomer. Measurements by Caritey on the average molecular weight of the HPG sample lead to the following: $M_w = 1.8 \times 10^6$ g/mol, which is an average degree of polymerization of about 3000, with a polydispersity index of about 1.55.[12] As its native polymer, guar gum, hydroxypropyl guar is expected to be a slightly stiffened, random-coil polymer. The hydrophobically modified hydroxypropyl guar, hm-HPG, is obtained by reaction of the HPG with a C_{22} *n*-alkyl epoxide. The number of hydrophobic substituents per individual polymer chain is expected to be 10. The measurement of the mean molecular weight and the polydispersity of associating systems like hm-HPG is difficult and it is assumed that the hydrophobic modification of HPG does not produce chain degradation.[12] The purity index is 95% (byproducts: propylene glycol, ethylene glycol, sodium acetate, open form of epoxide alkane).

The erucylbis(hydroxyethyl)methylammonium chloride (EHAC) is a C_{22} surfactant with a cis unsaturation at the 13-carbon position. Its chemical structure is shown below:

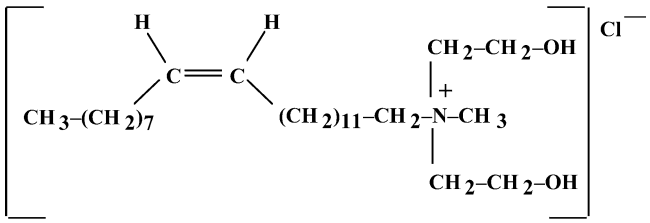

It is supplied by Akzo Nobel, Chemicals, LLC. It is used in the form of a liquid blend of the quaternary ammonium salt with 25 wt % 2-propanol (IPA). Upon dilution, the ratio IPA/EHAC is maintained constant. The concentrations of the EHAC samples reported in the text correspond to the active surfactant (i.e., after correction of the 25 wt % IPA added in the blend).

Potassium chloride was supplied from Aldrich.

Solutions containing surfactant and salt were prepared using deionized water. The concentration of polymer or surfactant will be expressed in wt %.

Methods. Rheological experiments were performed with a Bohlin CVO rheometer. Steady-state measurements were done under controlled stress or controlled rate depending on the sample viscosity, using the cup and bob geometry (coaxial cup, 25 mm diameter bob) or a double gap cell (inner diameter 40 mm, outer diameter 50 mm). The shear rate was varied between 10^{-3} and 2000 s^{-1}. The response of the shear viscosity as a function of time during the start up of a shear flow is characterized by a rather long equilibrium time, from 200 up to 1000 s, depending on the sample composition. A good reproducibility of the nonlinear rheological results was obtained without having to use a pre-shearing protocol.[5] Dynamic rheological experiments were carried out with the same rheometer using the coaxial cup cell. The frequency was varied between 10^{-3} and 5 Hz under a maximum shear stress of 1 Pa. The frequency spectra were conducted in the linear viscoelastic regime of the samples, as determined previously by dynamic stress sweep measurements. The cell was heated by a reservoir of fluid circulating from a high-temperature bath. A metallic cover was placed on the top of the sample to minimize sample evaporation. The sample was equilibrated for at least 15 min at each temperature prior to conducting experiments. Both steady and dynamic rheological experiments were performed at different temperatures.

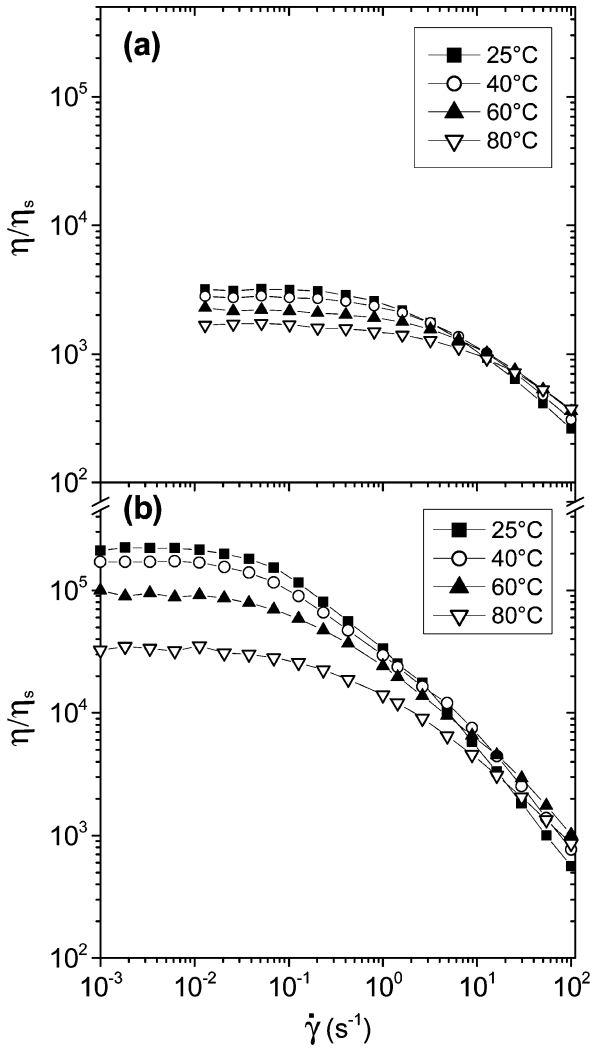

Figure 1. Relative steady-state viscosity vs shear rate for HPG (a) and hm-HPG (b) solutions at $C = 1$ wt %, in the presence of 0.4 M KCL, at various temperatures. The lines drawn through the data are guides for the eye.

Results

Comparison of the Flow Rheology of Hydrophobically Modified and Unmodified Hydroxypopyl Guars. Figure 1. shows typical variations of the steady-state values of the relative viscosity η/η_s where η_s is the solvent viscosity, as a function of the shear rate $\dot{\gamma}$ for a HPG sample and its hm-HPG homologue at $C = 1$ wt % and at various temperatures ranging from 25 to 80 °C. The relative zero-shear viscosity of the HPG solution, determined from the Newtonian plateau, is found to decrease significantly as the temperature is increased (Figure 1a). Moreover, the crossover between the Newtonian plateau and the shear-thinning regime is shifted to higher values of $\dot{\gamma}$. This indicates a speeding up of the dynamics of the system since the inverse of the shear rate at the crossover, $\tilde{\dot{\gamma}}^{-1}$, can be roughly identified with the terminal time $\boldsymbol{T}_R$ of the stress relaxation.

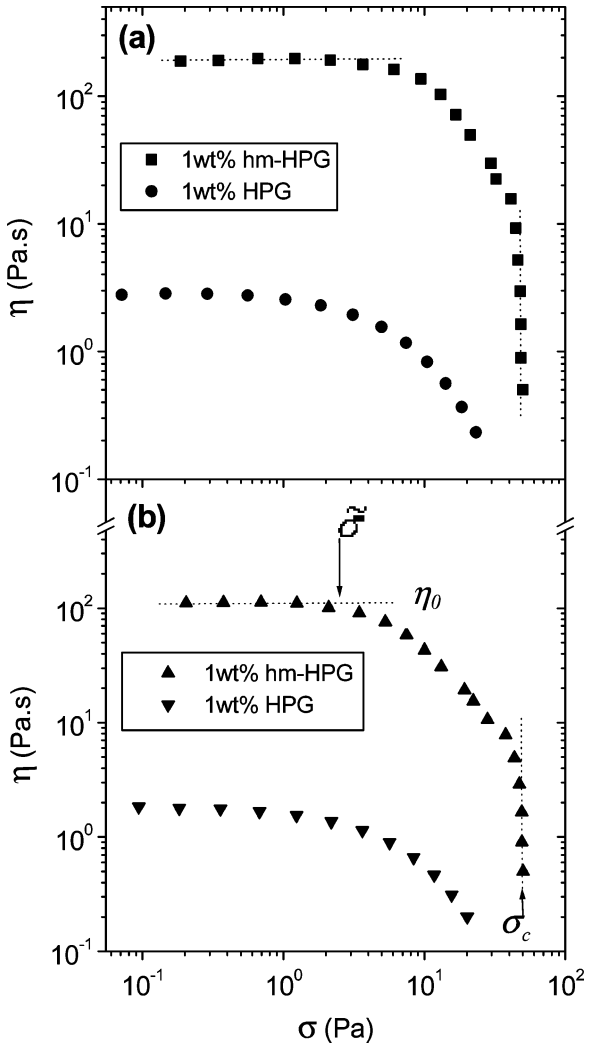

Figure 2. Steady-state shear viscosity vs shear stress for HPG and hm-HPG solutions in the presence of 0.4 M KCl at two different temperatures: (a) 25 °C; (b) 40 °C. η_0 is the Newtonian viscosity, $\tilde{\sigma}$ is the shear at the onset of shear thinning, and σ_c is the critical stress.

At high shear rates, the representative curves of $[\eta/\eta_s]$-$(\dot{\gamma})$ cross each other, so that the high shear value of the relative viscosity increases with temperature, that is the opposite behavior of that of the zero-shear viscosity. The overall behavior described above was observed over the concentration range investigated in this study (0.1 up to 3 wt %).

The same effects are observed for solutions of the modified hm-HPG polymers, as shown in the example of Figure 1b. In that case, the decrease of the zero-shear viscosity as the temperature is increased is much more pronounced. The $[\eta/\eta_s](\dot{\gamma})$ curves also cross each other in the same range of $\dot{\gamma}$ as for the unmodified polymer of similar concentration.

The effect of the polymer modification on the flow behavior is shown by comparing the data of Figure 1, parts a and b, respectively. The effect is that previously reported for systems in the entangled state.[5,8,41] In particular, the zero-shear viscosity is larger for the modified samples and the shear-thinning regime is shifted to lower values of $\dot{\gamma}$. This behavior is well taken into account by the sticky reptation model meant for entangled networks made up of linear chains with many temporary cross-links.[10,11] In this model, the chain

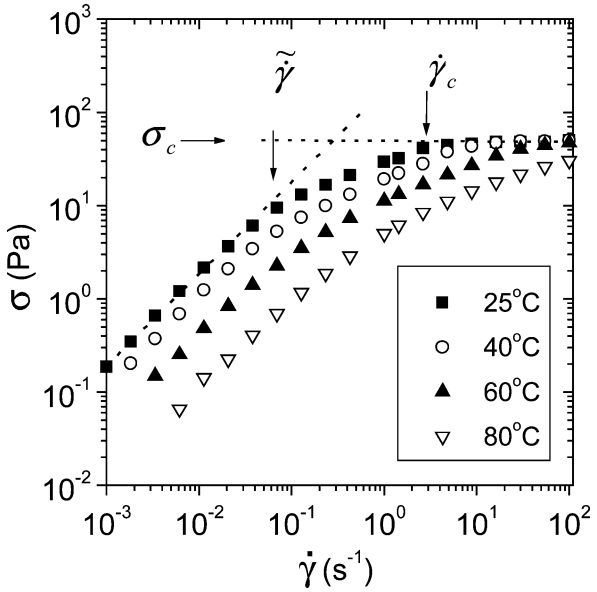

Figure 3. Shear stress vs shear rate for a 1 wt % hm-HPG solution at various temperatures. In the Newtonian regime at low shear rates, the data are fitted by a straight line of slope 1.

motion, governed by the reptation hindered by the hydrophobic interactions, is controlled by the concentration and the lifetime of the tie points.

Previously reported rheological experiments, carried out with a stress-controlled rheometer on the same systems revealed the presence of a discontinuity in the flow curves of the modified hm-HPG, occurring at a critical shear stress, σ_c, which increased with the polymer concentration.[5] This discontinuity was attributed to a breaking of the temporary hydrophobically associating network. Beyond the discontinuity, the flow curves of the modified and unmodified polymers were found to coincide.

Typical variations of the steady-state shear viscosity vs shear stress, obtained in the present study, are represented in Figure 2. For the modified polymers, three regimes can be identified in the variation of the viscosity vs shear stress. At low shear stress, one observes the Newtonian plateau, followed by a shear-thinning regime beyond a shear stress $\tilde{\sigma} \approx \eta_0 T_R^{-1}$ where T_R represents the longest time of the stress relaxation and η_0 the Newtonian viscosity. The sharp viscosity drop, occurring at higher shear stress, defines the critical shear stress σ_c. The shear rate $\dot{\gamma}_c$, measured just before the sharp drop is, according to Aubry and Moan, the inverse of the lifetime of the associations.[5] An alternative representation is given in plotting the shear stress vs the shear rate, as illustrated in Figure 3, which shows the results obtained for 1 wt % solution of hm-HPG at different temperatures. The determination of the shear rate at the crossovers between the different regimes provide estimates of $\tilde{\dot{\gamma}} \approx T_R^{-1}$ and $\dot{\gamma}_c$. The latter corresponds to the onset of the high shear plateau. It can be observed in Figure 3 that the critical shear stress is roughly independent of temperature at C = 1 wt %, whereas $\dot{\gamma}_c$ increases with temperature. The variation of σ_c with concentration (not shown here) can be fitted at T = 25 °C by a power law $\sigma_c \approx C^{1.62}$ in agreement with the previous findings of Aubry and Moan in the salt-free systems: $\sigma_c \approx C^{1.7}$.[5] As for $\dot{\gamma}_c$, it is found to decrease slightly upon increasing concentration ($\dot{\gamma}_c \approx 12$ s^{-1} for C = 0.35 wt % and $\dot{\gamma}_c \approx 3$ s^{-1} for C = 1

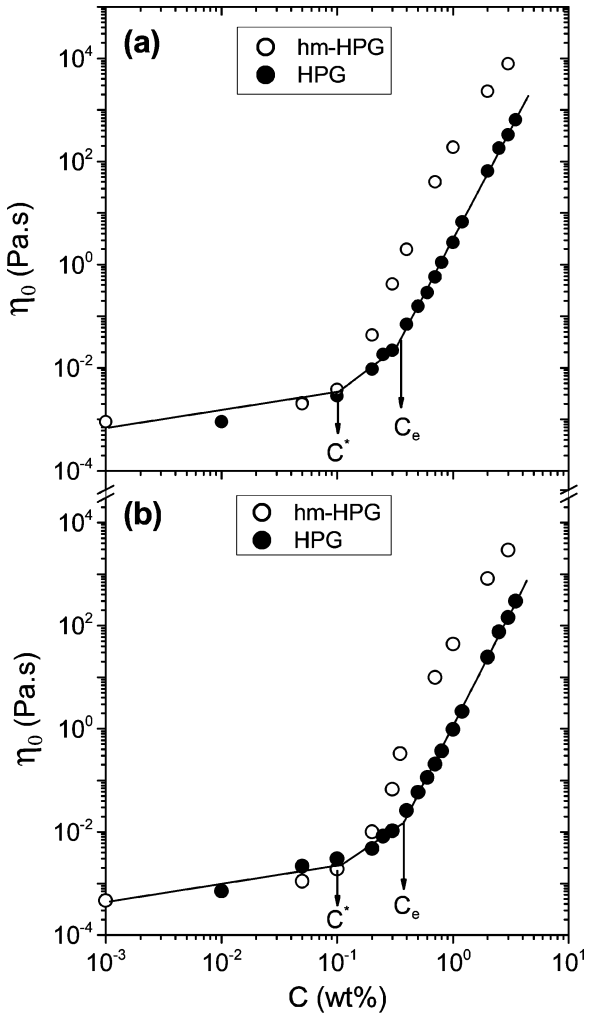

Figure 4. Variation of the zero-shear viscosity with concentration for solutions of HPG and hm-HPG in the presence of 0.4 M KCl: (a) $T = 25$ °C; (b) $T = 60$ °C.

wt % at $T = 25$ °C). It should be noted that, whereas σ_c can be determined with a good approximation, $\dot{\gamma}_c$ is less well-defined. As mentioned in the Experimental Section, the equilibrium value of the stress upon applying a steady strain is reached after a long time. The transient response curves of the stress are characterized for shear rates in the vicinity of $\dot{\gamma}_c$ by a large overshoot followed by a long relaxation. Such effects were reported for both wormlike micellar solutions[42−44] and hydrophobically modified polymers.[5,45]

It must also be remarked in Figure 1 that, in the whole shear rate range investigated, the steady-state viscosity of the modified sample remains larger than that of the unmodified one. This means that one does not reach the very short time scale where one probes local motions, insensitive to the presence of tie-points.

Figure 4 shows the comparison between the variations of the zero-shear viscosity vs polymer concentration measured at $T = 25$ °C and $T = 60$ °C for the HPG and hm-HPG samples, respectively.

For the unmodified polymer, one observes the classical behavior, with a first break at the concentration C^* at which the chains start to overlap and a second break at a higher concentration C_e corresponding to the onset of entanglements.[46−48] In this respect, it should be noted that a significant overlap of neighboring chains is required in order for them to constrain each other motion. As a consequence, the strand between two consecutive entanglements in a chain is composed of a number $\tilde{N}$ of blobs with a size ξ.[49,50] Both C^* and C_e and the exponent α of the asymptotic law obtained for the HPG sample in the entangled regime were found to be quite independent of the temperature within the experimental accuracy. Their values are given in Table 1. The ratio C_e/C^* is on the order of 3.5, that is a smaller value than those obtained for other systems, which range generally between 5 and 10.[47,48,50,51] In fact, there is no theoretical model which allows one to predict this ratio, which is likely to depend on the nature of the polymer and in particular on its natural persistence length.

Table 1. Crossover Concentrations C^* and C_e and Exponent α of the Scaling Law of the Zero-Shear Viscosity vs Concentration in Entangled Solutions of the Modified and Unmodified HPG Samples

polymer	C^* (wt %)	C_e (wt %)	C_e/C^*	α
HPG	0.10	0.35	3.5	4.4
Hm-HPG	0.15			

The rheological behavior of the modified polymers is quite different. The viscosity of the solution rises steeply beyond a concentration which is of the same order of magnitude as the crossover concentration C^* of the unmodified polymer (Figure 4 and Table 1). Such a behavior has already been reported for solutions of hydrophobically modified polyacrylamides.[7] In the latter case, clear Rouse regimes were observed and entanglement onsets could be determined. In the present case, there is no clear evidence of a Rouse regime in the curves of Figure 4, which display a sigmoidal shape.

Note that experiments performed by Aubry and Moan on the same system at 25 °C showed a behavior quite similar to that represented in Figure 4, with $\alpha = 4.3$ for the HPG polymers.[5]

Viscoelastic Behavior of EHAC/hm-HPG Mixtures. We have investigated the rheological behavior of mixtures with different compositions. The latter are characterized by the ratio $R = C_{EHAC}/(C_{EHAC} + C_{hm-HPG})$ where the concentrations of the components are expressed in wt %.

Figure 5 represents typical frequency dependences of the storage (G') and loss (G'') moduli for a mixture at an overall concentration $C_M = 0.35$ wt % and $R = 0.43$. A behavior, characteristic of entangled systems is observed, with a crossing of the $G'(\omega)$ and $G''(\omega)$ curves and a plateau modulus G_o at high frequencies. The relaxation time T_R and the plateau modulus G_o have been determined from the crossing point of the curves $G'(\omega)$ and $G''(\omega)$, according to $\omega_{max}T_R = 1$ and $G_o = 2G'(\omega_{max}) = 2G''(\omega_{max})$.

Figure 6 represents the variations of T_R and G_o with the mixture composition, for samples with an overall concentration $C_M \approx 0.35$ wt %. The compositions of the mixtures are the following:

$R = 0$: 0.35 wt % hm-HPG

$R = 0.2$: 0.3 wt % hm-HPG + 0.075 wt % EHAC

$R = 0.43$: 0.2 wt % hm-HPG + 0.15 wt % EHAC

$R = 0.69$: 0.1 wt % hm-HPG + 0.225 wt % EHAC

$R = 1$: 0.375 wt % EHAC

A maximum is observed in the relaxation time and to a lesser extent in the plateau modulus that is the signa-

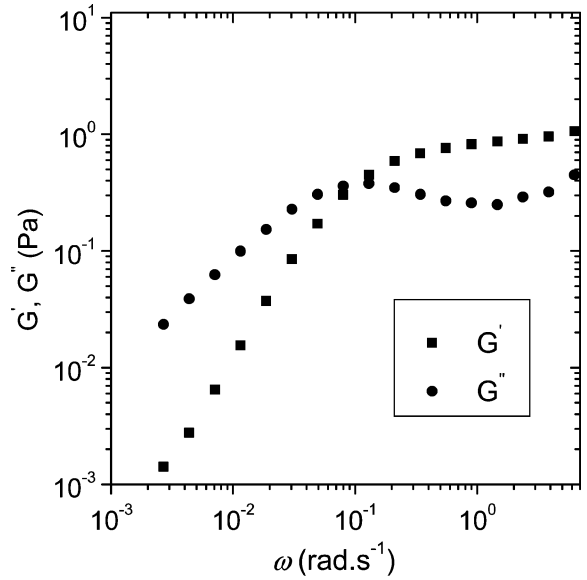

Figure 5. Storage (G') and loss (G'') moduli as a function of frequency at 25 °C for a solution of 0.2 wt % hm-HPG, 0.15 wt % EHAC, and 3 wt % KCl ($R = 0.43$).

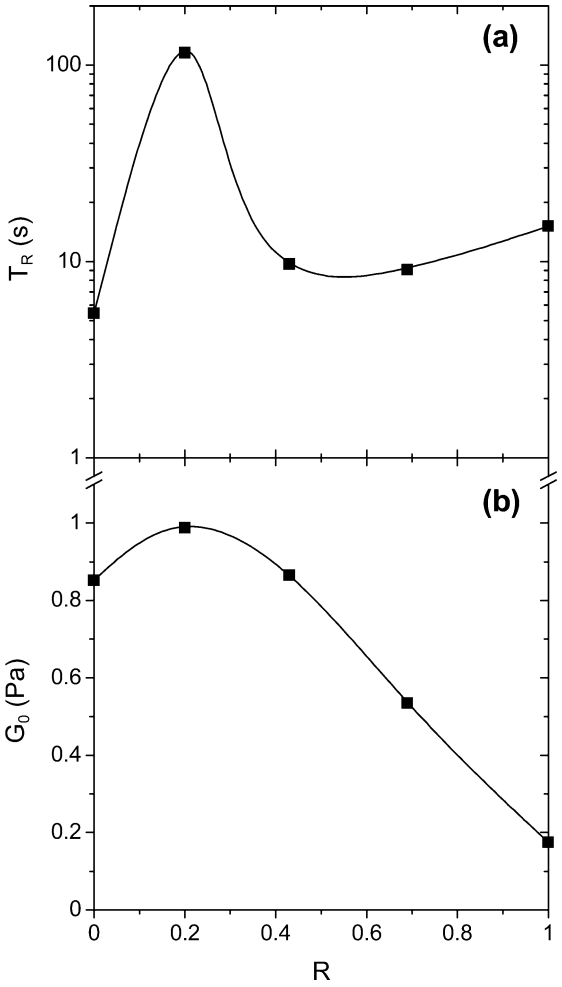

Figure 6. Terminal relaxation time (T_R, a) and plateau modulus (G_0, b) vs R for systems with an overall concentration $C_M \approx 0.35$ wt %.

ture of a pronounced synergy. The comparison between the plateau moduli of the EHAC and the hm-HPG solutions ($R = 1$ and $R = 0$ respectively) at about the same concentration shows that the density of the entanglements between the wormlike micelles is strongly reduced as compared with that of the cross-links and/or the entanglements of the associating polymers. Another interesting feature concerns the high-frequency range of the viscoelastic curves, which has never been analyzed before in associating polymer solutions. The minimum which is observed for G'' at the circular frequency ω_m corresponds to the crossover between the reptation controlled stress relaxation and the Rouse modes. The position and the normalized amplitude of the dip have been derived by Granek[52] and are given by

Table 2. Effect of the Mixture Composition on the Dip Coordinates ω_m and $G''(\omega_m)/G_0$ for Solutions with Overall Concentrations $C_M \approx 0.35$ wt % at 25 °C

R	ω_m (rad. s^{-1})	$G''(\omega_m)/G_0$
0	2.3	0.33
0.2	0.6	0.16
0.43	1.2	0.29
0.69	1.9	0.17
1	1.1	0.35

$$G''(\omega_m)/G_0 \sim (l_e/L)^{4/5} \quad (1)$$

$$\omega_m \sim \left(\frac{l_e}{L}\right)^{4/5} \tau_e^{-1} \quad (2)$$

where L is the contour length of the chain, l_e is the entanglement length, and τ_e is the Rouse time of the entanglement length. The above relations are valid for the regular polymers and the wormlike micelles, providing that the dip occurs at frequencies much higher than the inverse of their breaking time. This was found to be the case for EHAC solutions.[20] For associating polymers, it can be speculated that eqs 1 and 2 can be applied, providing that ω_m is much larger than the inverse of the lifetime of the associations. Also, it should be kept in mind that the Rouse part of the spectrum may be modified by the breaking mechanism of the associations.

Table 2 gives the effect of the mixture composition on the values of ω_m and $G''(\omega_m)/G_o$ for systems with an overall concentration $C_M \approx 0.35$ wt %, at $T = 25$ °C. The dependence of these parameters on R is rather complex but a clear minimum of both ω_m and $G''(\omega_m)/G_o$ is observed for $R = 0.2$, again suggesting a synergistic effect at this composition.

The variations of the zero-shear viscosity of different EAHC/hm-HPG mixtures vs hm-HPG and EHAC concentrations, at 25 °C, are plotted in Figure 7, parts a and b, respectively. A net zero-shear viscosity enhancement is observed in both representations by addition of one component to the other. Synergistic effects are best revealed by the plots of the zero-shear viscosity vs the total material concentration C_M (wt %), at various temperatures (Figure 8). At 25 °C, there is a clear synergy for the zero-shear viscosity in a range of concentrations between 0.07 and 1 wt % (Figure 8a). As an example, at a concentration $C = 0.37\%$, for which both EHAC and hm-HPG solutions have the same viscosity ~ 2 Pa·s, the viscosity of the mixtures is about 5 Pa·s for $R = 0.69$, 9.2 Pa·s for $R = 0.43$ and 83 Pa·s for $R = 0.2$. The synergystic effect can also be expressed in the following way: to obtain a viscosity of 10 Pa·s, one can use either 0.6% solutions of pure EHAC or pure hm-HPG or 0.23 wt % solutions of mixtures (for instance 0.18 wt % of hm-HPG + 0.05 wt % of EHAC). In the high concentration range, all the variations of η_0 with

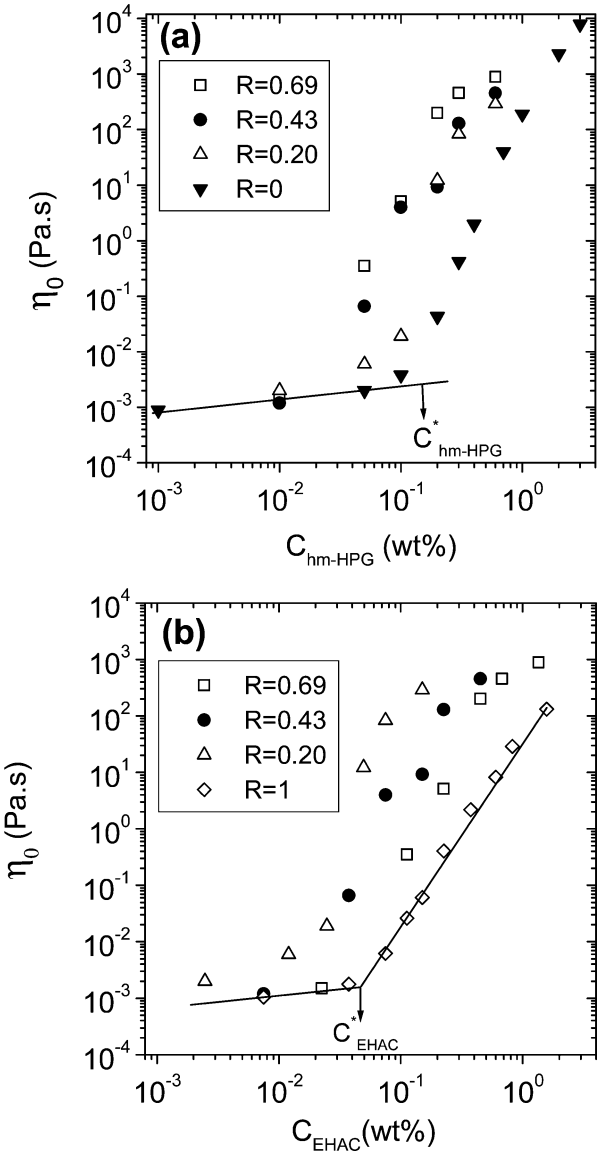

Figure 7. Zero-shear viscosity vs hm-HPG (a) and EHAC (b) concentrations for various compositions of the mixtures at 25 °C. Also are reported the variations corresponding to the single hm-HPG and EHAC components, respectively.

Table 3. Effect of the Mixture Composition on the Parameters σ_c and $\dot{\gamma}_c$ for Solutions with an Overall Concentration $C_M \approx 0.35$ wt % at Various Temperatures[a]

R	T (°C)	σ_c (Pa)	$\dot{\gamma}_c$ (s^{-1})
0	25	8.5	12
	40	7.7	36
	60	4	150
0.2	25	2.5	1.6
	40	3.5	9
	60	5.5	27
0.43	25	5.8	39
	40	5.8	70

[a] The critical shear stress σ_c and critical shear rate $\dot{\gamma}_c$ are measured with an accuracy of ±10% and ±25% respectively.

C_M tend to converge and there is no longer synergy. The results obtained at $T = 40$ °C are quite similar, whereas at 60 °C the viscosity enhancement with respect to the hm-HPG solutions is more limited. Finally at $T = 80$ °C, mixtures with $R \leq 0.43$ exhibit the same viscosity as the hm-HPG for $0.15\% < C_M < \sim 0.7\%$ whereas at higher concentrations, the value of the zero-shear viscosity is between those of the hm-HPG and the EHAC samples.

A more illustrative description of this synergistic effect is provided by Figure 9 where the zero-shear viscosity is plotted as a function of the composition R, for various temperatures and for systems with an overall concentration $C_M \approx 0.35\%$, that is about 2.3 times the C^* of the modified polymer. The maximum which is observed for $R = 0.2$ at all temperatures up to 80 °C is the signature of the synergy, the latter being more pronounced at low temperature. Figure 10 shows the flow curves obtained for systems with $C_M \approx 0.35\%$, which is the concentration in the optimal range with respect to the synergy. This synergy, which appears in the Newtonian plateau, is also reflected by the behavior of $\tilde{\dot{\gamma}}$ that corresponds to the onset of the shear thinning and is on the order of T_R^{-1}. In fact, the values of $\tilde{\dot{\gamma}}$ observed in the curves of Figure 10 for $T = 25$ °C correspond approximately to the values of T_R obtained from the linear viscoelasticity measurements and reported in Figure 6. The only exception concerns the hm-HPG sample for which one observes a Newtonian plateau much larger than what can be expected from the linear viscoelastic measurement ($\tilde{\dot{\gamma}}^{-1} = 0.1$ s as opposed to $T_R \approx 5$s). Significant deviations from the relationship $\tilde{\dot{\gamma}}^{-1} = T_R$ were also reported for other hydrophobically modified water-soluble polymers.[7,40,53,54] In the present case, a close inspection of the flow curve obtained at $T = 25$ °C for the hm-HPG solution reveals a weak shear-thickening. This effect which is commonly observed for associating polymers in the vicinity of C^* masks the real onset of shear thinning.[1,41,55,56]

The variation of $\eta(\dot{\gamma})$ for mixtures of different R also shows that the composition dependent synergistic effects are maintained at least up to $\dot{\gamma} = 100$ s^{-1}. This is illustrated in Figure 11 where the viscosity at $\dot{\gamma} = 100$ s^{-1} is plotted vs R for systems with an overall concentration $C_M \approx 0.35\%$ and at various temperatures. A maximum is observed for $R = 0.2$, the amplitude of the maximum being roughly temperature independent. In fact, the viscosity at $\dot{\gamma} = 100$ s^{-1} is only weakly temperature dependent, whatever the composition of the system. For instance, for the system with $R = 0.2$, the viscosity $\eta_{100\ s^{-1}}$ drops by a factor of ~ 2 between 25 and 80 °C.

In Figure 12 are reported the same flow curves as those of Figure 10, in the representation $\eta = f(\sigma)$. The behavior of the blends is more complex than for the single component EHAC or hm-HPG solutions. The high shear viscosity of mixtures still exhibits a more or less sharp drop, depending on the composition and the temperature. For systems with a well-defined plateau, one can determine the values of both σ_c and $\dot{\gamma}_c$. The values thus obtained are reported in Table 3. Inspection of this table reveals several features. First, the decrease of σ_c upon increasing temperature for the hm-HPG solutions is much stronger than at higher concentration (cf. Figure 3). Second, whereas the behavior of σ_c is rather complex, $\dot{\gamma}_c$ presents a pronounced minimum at the composition $R = 0.2$ corresponding to the optimal synergistic effect. If, as stated by Aubry and Moan, $\dot{\gamma}_c$ represents the inverse of the lifetime of the temporary cross-links, this means that the lifetime of a EHAC/hm-HPG mixture with $R = 0.2$ is much larger (1.6 s at 25 °C) than that of the pure hm-HPG at the same concentration (0.08 s at 25 °C).[5]

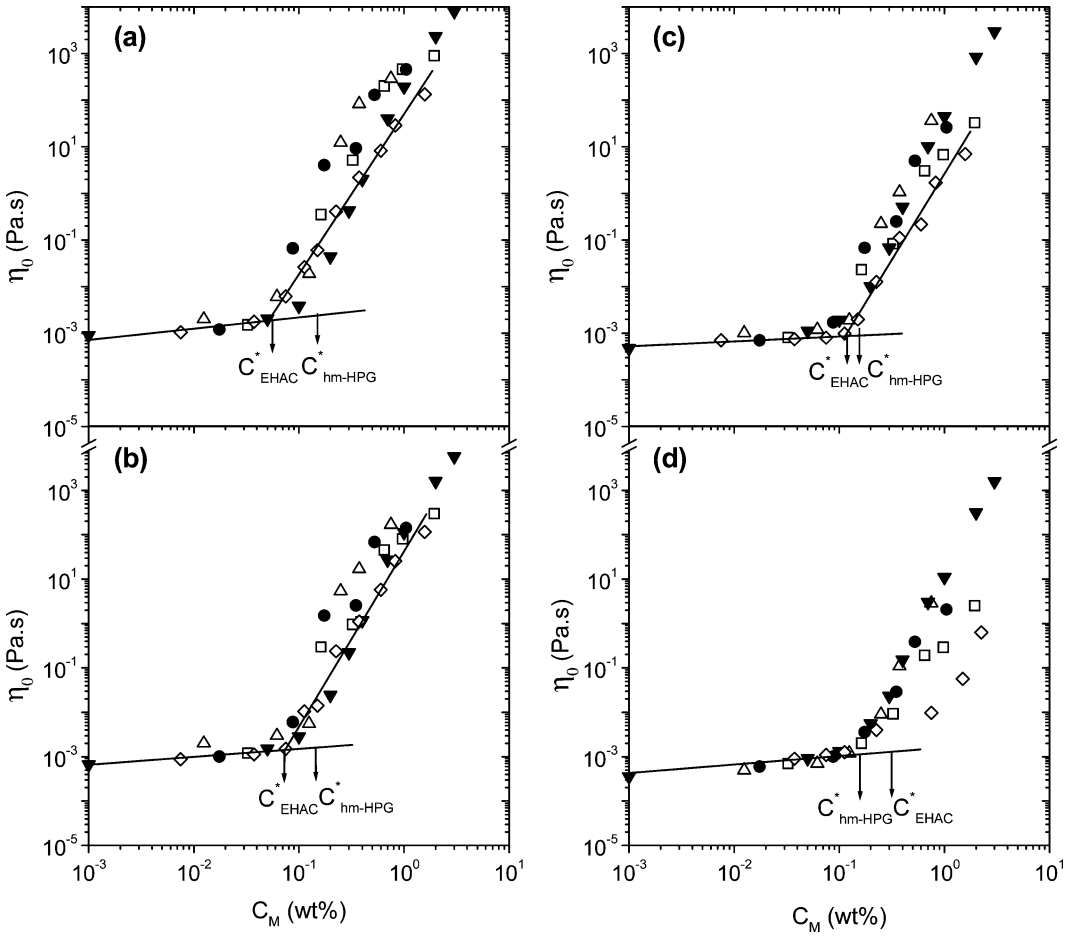

Figure 8. Zero-shear viscosity vs overall concentration for various compositions of the mixtures [(▼) $R = 0$, (△) $R = 0.2$, (●) $R = 0.43$, (□) $R = 0.69$, (◇) $R = 1$] at various temperatures: (a) $T = 25$ °C; (b) = 40 °C; (c) $T = 60$ °C; (d) $T = 80$ °C.

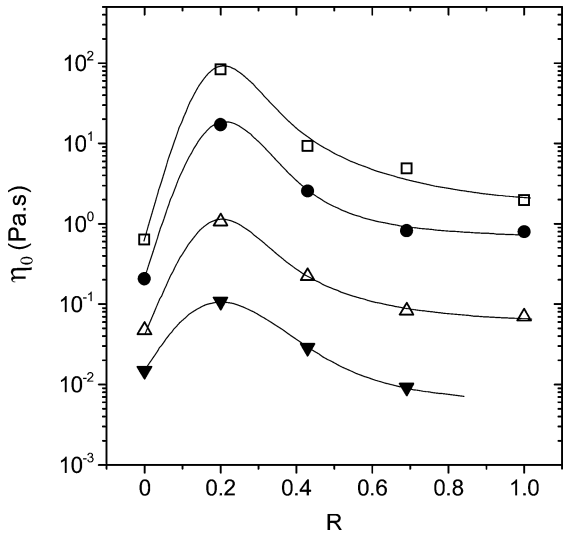

Figure 9. Zero-shear viscosity vs R at various temperatures: (□) 25 °C; (●) 40 °C; (Δ) 60 °C; (▼) 80 °C. Data are for systems with $C_M \approx 0.35$ wt %. The lines drawn through the data are guides for the eye.

Discussion

Unmodified and Modified Guars. We discuss first the behavior of the unmodified polymer. The guar is a slightly stiffened random coil polymer for which one can use the methods commonly employed in synthetic polymer studies.[57] In particular, the crossover volume fraction ϕ^* can be written as

$$\phi^* \approx \frac{SL}{R_g^3} \tag{3}$$

where S is the section of the chain and R_g the radius of gyration. According to both the classical Flory's theory and the scaling model developed by de Gennes, the expression of ϕ^* for a flexible chain with N monomeric units of size a and a persistence length l_p, under good solvent conditions, is given by[46]

$$\phi^* \approx S l_p^{3/5} v_0^{-3/5} L^{-4/5} \tag{4}$$

$$\phi^* \approx a^{6/5} l_p^{3/5} v_0^{-3/5} N^{-4/5} \tag{5}$$

where v_0 is the excluded volume parameter.

In the semidilute regime, $C \geq C^*$, the solution can be viewed as a melt of blobs whose size is the correlation length ξ, which, according to the scaling model of de Gennes is given by[46]

$$\xi \approx a^{3/2} l_p^{1/4} v_0^{-1/4} \phi^{-3/4} \tag{6}$$

On the basis of the static picture outlined above, a dynamical scaling model has been proposed. In the entangled regime, the dynamical properties depend on the spatial scale. For length scales shorter than the correlation length, the hydrodynamic interactions control the dynamics and the motion within the blobs is Zimm-like, with a characteristic relaxation time τ_ξ

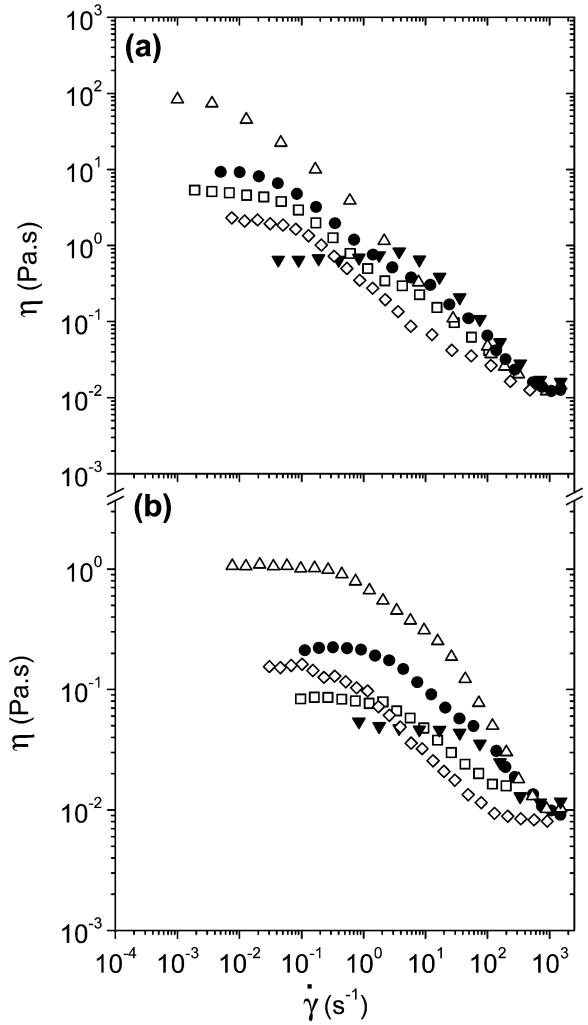

Figure 10. Variation of the steady shear viscosity as a function of shear rate for different R values [(▼) $R = 0$, (△) $R = 0.2$, (●) $R = 0.43$, (□) $R = 0.69$, (◇) $R = 1$] with $C_M \approx 0.35$ wt % at two temperatures: (a) 25 °C; (b) 60 °C.

proportional to the blob volume ξ^3

$$\tau_\xi \approx (\eta_s/kT)\xi^3 \tag{7}$$

On distance scales larger than ξ, the behavior is that of a Rouse chain formed of $\widetilde{N}$ blobs. Finally, the dynamics associated with the $N/(\widetilde{N}\phi\xi)^3$ entanglement strands is reptation-like.

Under these assumptions, the longest relaxation time is given by[46,58]

$$T_R \approx \tau_\xi \widetilde{N}^2[N/(\widetilde{N}\phi\xi^3)]^3 \tag{8}$$

$$T_R \approx (\eta_s kT)\widetilde{N}^{-1}N^3\phi^{-3}\xi^{-6} \tag{9}$$

The zero-shear viscosity is given by

$$\eta_0 = T_R G_0 \tag{10}$$

where G_0 is the plateau modulus which is proportional to the entanglement density

$$G_0 = kT/(\widetilde{N}\xi^3) \tag{11}$$

It follows that

$$\eta_0 \approx \eta_s \widetilde{N}^{-2}N^3\phi^{-3}\xi^{-9} \tag{12}$$

Equation 12 shows that, at a given concentration, the zero-shear viscosity varies oppositely to the correlation length.

The experimental observation of a decrease of the relative zero-shear viscosity η_0/η_s upon increasing the temperature (cf. Figure 1) suggests then an increase of the correlation length with temperature and correspondingly a decrease of the excluded volume parameter (cf. Equation 6), that is a decrease of the quality of solvent. The latter might result from the breaking of the hydrogen bonds present in most aqueous solutions of hydrophilic polymers. A decrease of v_0 upon increasing the temperature should lead to an increase of C^*, according to eq 4. However, this effect is much weaker for C^* that varies like $v_0^{-3/5}$ than for η_0/η_s that scales like $\xi^{-9} \sim v_0^{9/4}$ (eqs 6 and 12). Experimentally no significant variation of C^* with temperature could be detected. Since η_0/η_s only decreases by a factor of ~ 2 when T varies from 25 to 80 °C, the expected variation of C^* remains in the limit of the experimental accuracy. Note that a possible effect of temperature on the persistence length may also be invoked.

The high shear results are also in agreement with the above observations. At high shear rate, the flow is controlled by the Zimm-like dynamics within a blob (cf. eq 7). In that limit, for a system at a given concentration, the high shear viscosity should increase with ξ. This might explain the crossing of the curves $[\eta/\eta_s](\dot{\gamma})$ observed in Figure 1a, leading to an increase of the high shear rate viscosity with temperature.

Looking now at the concentration dependence of the zero-shear viscosity, one obtains power laws with an exponent on the order of 4 (Figure 4). This is the classical behavior of random coils in good solvent and is in agreement with the scaling model that predicts:[46,58]

$$\eta_0 = \eta_s \widetilde{N}^{-2}N^3\phi^{15/4} \tag{13}$$

The above equation is obtained by inserting the scaling law $\xi \approx \phi^{-3/4}$ in eq 12.

The behavior of the modified polymer, as compared to that of the unmodified one, is quite similar to that reported for other systems. The enhancement of the zero-shear viscosity is accounted for by the sticky reptation model developed first by Leibler et al.[10] and subsequently by Rubinstein and Semenov.[11] The prediction of the first version of the sticky reptation model, for the zero-shear viscosity is

$$\eta_0 \approx \phi^{15/4}N^{7/2}[s]^2\tau(1 - 9/p + 12/p^2)^{-1} \tag{14}$$

where $[s]$ is the molar ratio of stickers with respect to the total number of monomers, p the average fraction of stickers engaged in an association, and τ the average lifetime of a sticker in a cross-link. The temperature dependence observed in Figure 1 for η_0/η_s is stronger than for the HPG sample (decrease of 6.5 compared to 2) and can be mainly ascribed to a decrease of the lifetime of the associations, as shown by the $\dot{\gamma}_c$ values reported in Table 3.[40]

The above prediction was obtained within the assumption that after the breaking of an association, the search of a sticker for a new partner is restricted to a part of the tube confining entangled chains. Rubinstein

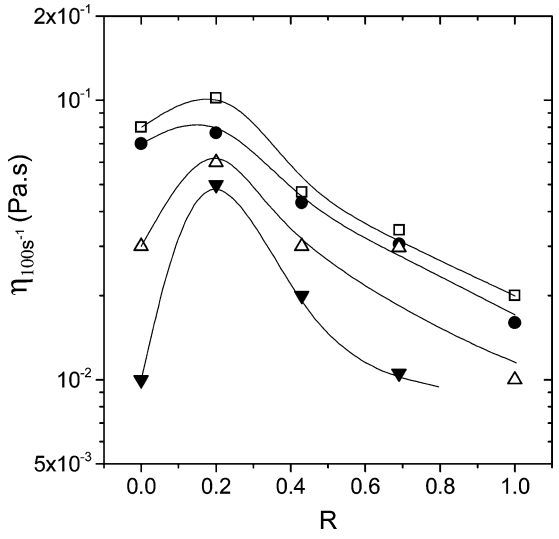

Figure 11. High shear rate viscosity vs R at various temperatures: (□) 25 °C; (●) 40 °C; (△) 60 °C; (▼) 80 °C. Data are for systems with $C_M \approx 0.35$ wt %. The lines drawn through the data are guides for the eye.

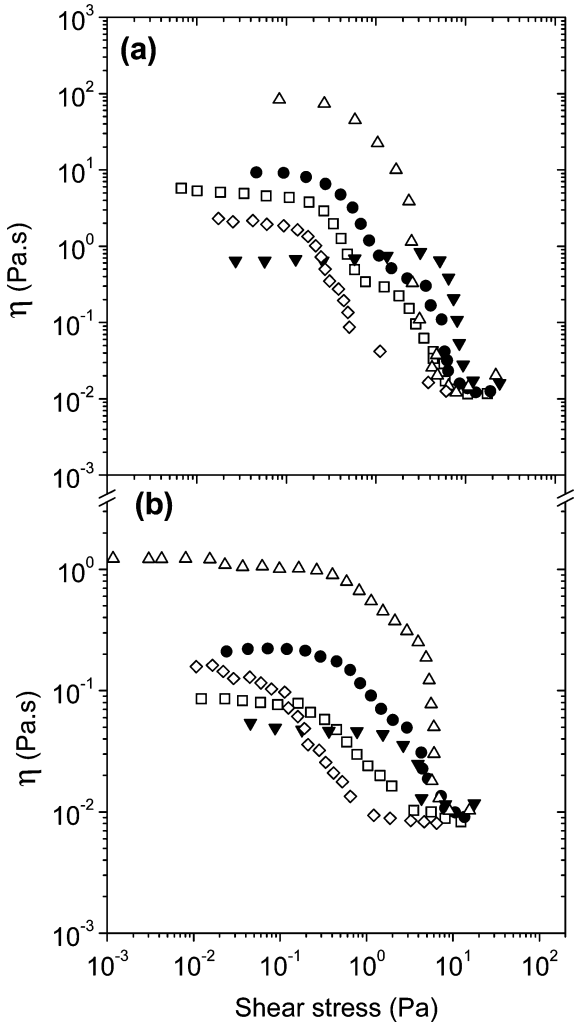

Figure 12. Variation of the steady shear viscosity as a function of shear stress for different R values [(▼) $R = 0$, (△) $R = 0.2$, (●) $R = 0.43$, (□) $R = 0.69$, (◇) $R = 1$] with $C_M \approx 0.35$ wt % at two temperatures: (a) 25 °C; (b) 60 °C.

and Semenov considered the effect associated with the increase of the fraction of the interchain associations at the expense of the intrachains ones with increasing the polymer concentration.[11] The model taking into account this effect predicts a very complex behavior of the zero-shear viscosity for entangled systems in good solvent with four successive regimes of different extent where the zero-shear viscosity varies with concentration according to power laws with exponents 6.8, 8.5, 3.7, and 4.7, respectively. This confers the representative curve of $\eta_0(C)$ a sigmoidal shape such as that observed experimentally in Figure 4.

In the high shear rate regime, the flow behavior is qualitatively the same as for the unmodified polymers, as illustrated by the comparison between Figure 1, parts a and b. A crossing of the curves $[\eta/\eta_s](\dot{\gamma})$ is again observed for the hm-HPG sample at about the same values of the crossing shear rates measured in Figure 1a.

EHAC/hm-HPG Mixtures. The synergistic behavior revealed by the rheological experiments is the signature of strong interactions between EHAC wormlike micelles and hm-HPG associating chains. These interactions are confirmed by the fact that the increase of the zero-shear viscosity occurs at an overall concentration on the order of C^*_{EHAC} and, depending on the temperature, smaller or equal to C^*_{hm-HPG}. Looking separately at the two components in the mixtures, it can be observed in Figure 7, parts a and b, that at $T = 25$ °C, the viscosity rise starts at EHAC and hm-HPG concentrations significantly lower than their respective C^*. Under these conditions, the EHAC micelles are shorter than at C^*, since their average length increases with concentration, in contrast with the polymer chains whose length remains unchanged. It should also be noted that the C^* of both hm-HPG and EHAC samples are of the same order of magnitude. It follows that the EHAC micelles, which are much thicker than the polymeric chains, are also longer in the vicinity of C^* according to eq 4.

The frequency dependences of the complex shear modulus provided by the linear viscoelasticity experiments are characteristic of entangled solutions, as ascertained by the presence of a plateau modulus and of a dip of $G''(\omega_m)$ in the high-frequency range. Therefore, the stress relaxation is controlled by the chain reptation. The ratio C/C^* of the investigated systems are of about 2.3 for the hm-HPG solution and about 7 for the EHAC and mixtures solutions ($T = 25$ °C). It should be noted that the viscoelastic curves are not significantly smeared by the polydispersity of the samples containing micelles and chains with very different lengths. However, it must be remembered that the terminal time of the stress relaxation of wormlike systems does depend not only on their length but also on their breaking time. In the limit where the breaking time is much shorter than the reptation time, the stress relaxation is described by a single exponential.[59] As for the relaxation time of associating polymers, it also depends both on their length and the lifetime of the associations. In any case, the reptational mechanism of these mixtures must be very complex, but surprisingly, the viscoelastic curves exhibit a quite simple behavior.

The nonlinear behavior of polymers and wormlike micelles submitted to a steady shear has been theoretically studied by Spenley et al.[60] The predictions of the model are the following: as the shear reaches a threshold value, $\dot{\gamma}_c = 2.6/T_R$, a mechanical instability of shear banding type occurs within the solutions. This instability is characterized above $\dot{\gamma}_c$ by a plateau of the shear

stress $\sigma_c = 2G_0/3$ (or a vertical variation in the representation $\eta(\sigma)$). The plateau persists over a finite $\dot{\gamma}$ range, beyond which there is again a linear increase of σ. In the plateau regime, bands of highly sheared liquid of high viscosity coexist with a more viscous part supporting a lower rate. Such a behavior does not seem to have been observed for ordinary polymers. Typically, some shear thinning occurs, but the shear stress continues to rise gently, reflecting a gradual stretching and orientation of the chains. This is what is observed in Figure 2 for the nonmodified HPG polymer.

The occurrence of a stress plateau and of a shear banding at high shear has been reported for wormlike micelles.[42−44] However, a true discontinuity of the slope in the $\sigma(\dot{\gamma})$ or $\eta(\sigma)$ curves only occurs at relatively high concentrations ($C/C^* \geq 15$). Below this value of C/C^*, the plateau regime is much smoother and rounded. As the concentration decreases, the plateau disappears with an inflection point as the only reminiscence. This regime corresponds to a progressive and homogeneous orientation of the micelles submitted to shear. This type of behavior is observed in the curves of Figure 12, parts a and b.

No model has been developed to describe the nonlinear flow behavior of hydrophobically modified polymers. Both our results and those of Aubry and Moan show the existence of an intermediate regime between the Newtonian one and the shear stress plateau, likely associated with stretching and orientation of the chains (cf. Figure 1).[5] The shear stress plateau might still be the signature of a shear banding instability. In order for the instability to occur, the cross-links between the associative units must be broken, and therefore the limiting step in the process will be controlled by the lifetime of the junction points, in agreement with the conclusions of Aubry and Moan.[5] The nonlinear rheology of the mixtures of EHAC and hm-HPG systems presents qualitatively the same features as those of hm-HPG polymers. It should be noted that the occurrence of a stress plateau was also recently reported by English et al. for hydrophobically modified alkali-swellable emulsion (HASE) polymers.[61] Contrary to the systems investigated here, addition of a high HLB surfactant tends to progressively diminish the shear-induced structuring.

Turning back to the synergistic effect, both linear viscosity and flow experiments show that for an overall concentration $C_M \approx 0.35$ wt % and $T = 25$ °C, the synergy is optimal for a composition of $R = 0.2$, as revealed by the maximum in T_R and η_0. Such a maximum can result from an increase of the micellar length, of the number and/or the lifetime of the temporary cross-links, or also from both effects.

The normalized amplitude and the position of the dip of $G''(\omega)$ given in Table 2 exhibit a minimum for $R = 0.2$. However, the comparison of Tables 2 and 3 shows that for all systems, except the one with the composition $R = 0.2$, $\omega_m \ll \dot{\gamma}_c$, so that the validity of eqs 1 and 2 is questionable. Still, these results confirm the specific behavior of the mixture with $R = 0.2$.

As for the variation of the critical shear rate with R reported in Table 3, it exhibits a minimum for the composition $R = 0.2$, suggesting a maximum of the lifetime of the cross-links at this composition. As for the temperature dependence of $\dot{\gamma}_c$, it follows an Arrhenius behavior (results not shown here) from which an activation energy E_a can be determined. This activation energy is found to be $E_a = 24kT$ for $R = 0$ (hm-HPG), $E_a = 26.7kT$ for $R = 0.2$ and $E_a = 12.1kT$ for $R = 0.43$ (determination from two data points). This result shows an enhancement of the activation energy for the lifetime of the associations at the synergistic composition $R = 0.2$.

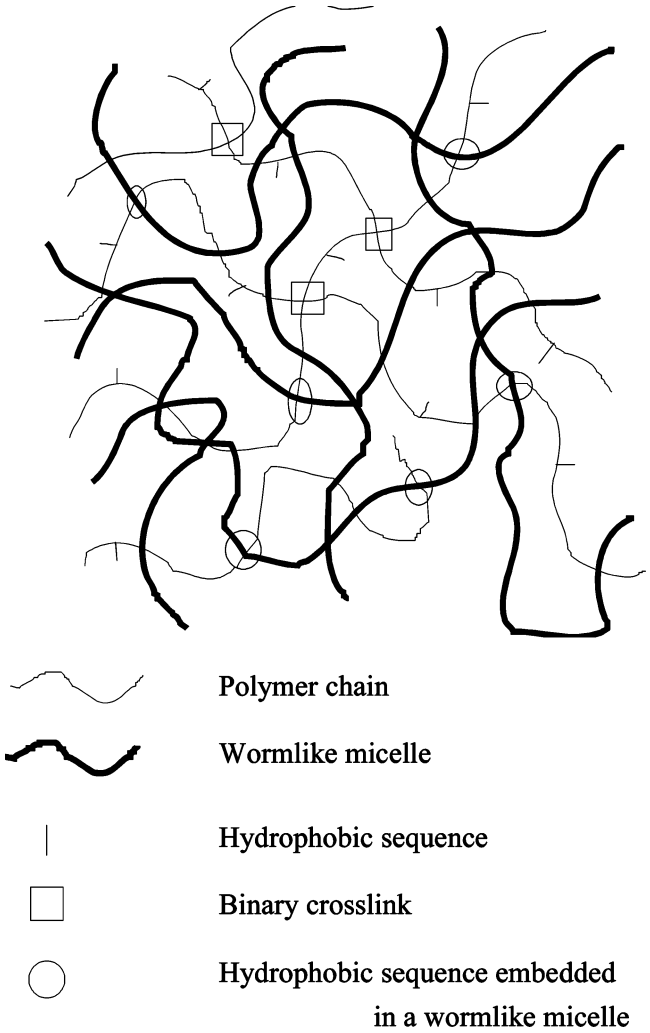

Figure 13. Interpenetrated network of wormlike micelles and hydrophobically modified chains of hm-HPG.

Three interaction mechanisms between micelles and associating polymers can be envisioned:

(i) The presence of surfactant produces a strengthening of the hydrophobic interactions through a noncooperative bonding. Recent studies have shown that the viscosity enhancement mostly results from a process where the surfactant decorates the preexisting cross-links and increases their lifetime.[34] However, this effect occurs for surfactant concentrations close to the cmc and disappears in the presence of an excess of surfactant. In the latter limit, it is generally believed that the hydrophobic sequences are singly solubilized by the spherical surfactant micelles.

(ii) The incorporation of hydrophobic sequences within the wormlike micelles produces a micellar growth, thus increasing the viscosity of the system.

(iii) Bridges are formed between the wormlike micelles and the hydrophobic sequences of the polymer to build a temporary network.

Considering the very large excess of surfactant concentration with respect to the hydrophobic sequences, a contribution arising from a decoration by the surfac-

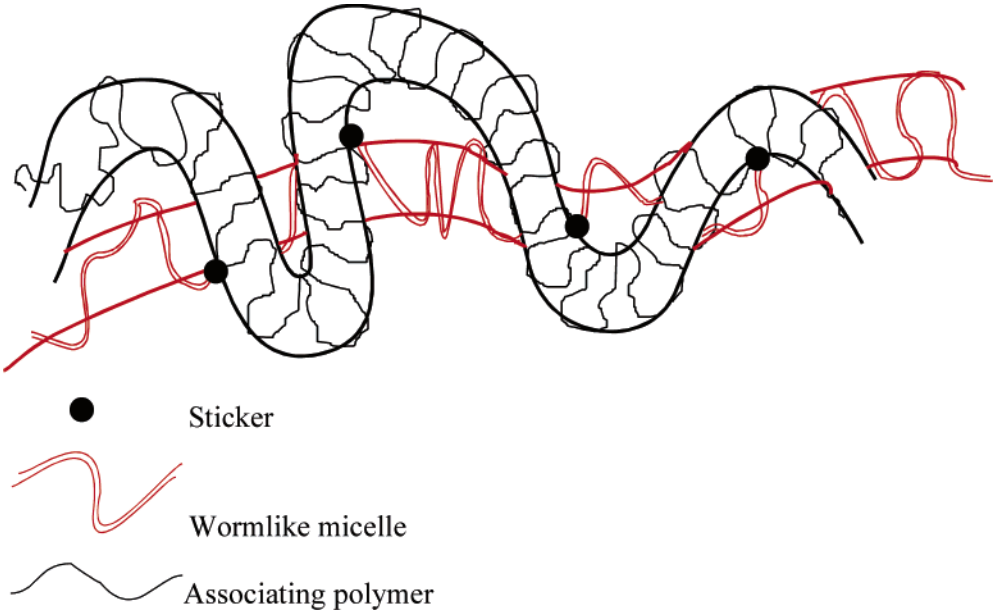

Figure 14. Representation of an associating polymer chain and a wormlike micelle in their respective tubes.

tant of preexisting cross-links must be ruled out. On the other hand, the formation of an interpenetrated network of wormlike micelles and hydrophobically modified chains, as schematized in Figure 13 might explain the viscosity enhancement. In such a scheme, most of the hydrophobic sequences are embedded within the wormlike micelles and possibly some binary (or multiple) cross-links are still present with also some free stickers. The scheme of Figure 13 represents a situation of entangled chains corresponding to an overall concentration C_M significantly larger than C^*_M.

The coupled motion in such systems can be described by the sticky Rouse model in the vicinity of C^*_M or by the sticky reptation model in the entangled state.[11,62] The latter case is illustrated by Figure 14, which represents one associating chain and one wormlike micelle in their respective tubes whose diameter is given by the average mutual entanglement length. Some stickers of the polymer chain are embedded in the wormlike micelle. In its reptation motion, the wormlike micelle can diffuse more or less freely within its tube despite the stickers, as the surfactant molecules can move without dragging the sticker. On the other hand, the polymer motion is somewhat hindered by the residency time of the sticker within the micelle, which is likely dependent on the micelle lifetime.

Experimentally, one observes a lesser or suppressed synergy at high concentration or at high temperature. In the high concentration regime, one might expect that the density of cross-links between the stickers increases. The effect of these cross-links possibly overcomes that of the stickers embedded in the micelle. Also, there may be some intermicellar branching that reduces the viscosity.[63] At high temperature, the micelles become much shorter. Therefore, the contribution to the viscosity from the wormlike micelles is decreased. Moreover, at high temperature, the micelles might become short enough not to make any longer bridges between the polymer chains. In this limit, the surfactant will only decorate the hydrophobic sequences and the viscoelastic behavior should tend to that of the unmodified polymer at the concentration of the modified polymer in the mixture.

Conclusion

This is the first report, to our knowledge, of synergystic effects in mixtures of hydrophobically modified polymers and wormlike micelles. The synergy manifests itself both in the linear and nonlinear properties of the systems. In particular, the zero-shear viscosity of the mixtures is significantly increased with respect to that of each component in an overall concentration range extending from 0.07 to 1 wt % and for temperatures up to 60 °C.

The combination of linear and nonlinear rheological measurements allowed us to show that the synergy results from an increase of the lifetime of the cross-links, which suggests the formation of cross-links between the micelles and the polymer chains. These results open new prospects both from fundamental and applied points of view. For thickening applications, the curves of Figures 7 and 8 and the comments given in the same section clearly show that it might be advantageous to replace the wormlike micellar systems or the modified polymers by a lesser amount of a mixture of these two components. This is reflected by the viscosity behavior at both low and high shear rates. Of particular interest is the presence of a maximum in the curves of Figure 11. This maximum shows that even at $T = 80$ °C and $\tilde{\dot{\gamma}} = 100s^{-1}$, an appreciable viscosity of about 0.05 Pa·s can be obtained with an appropriate mixture, which make these systems useful as fracturing fluids.

Several issues concerning the fundamental properties are still open. The schemes proposed to explain the rheological behavior of these systems are very qualitative and a real model describing the coupled flow of wormlike micelles and hydrophobically modified polymers is lacking. The experimental observation that the synergy takes place in a limited range of overall concentrations is not easily explainable. More results on both linear and nonlinear properties of another modified polymer−wormlike micelle system will be presented in a forthcoming paper.

Acknowledgment. The authors wish to thank J. S. Candau (ULP, Strasbourg, France) and J. Selb (ICS, Strasbourg, France) for helpful discussions.

References and Notes

(1) Glass, J. E., Ed. *Polymers in Aqueous Media: Performance through Association*; Advances in Chemistry 223; American Chemical Society: Washington, DC, 1989.
(2) Glass, J. E., Ed. *Hydrophilic Polymers: Performance with Environmental Acceptability*; Advances in Chemistry 248; American Chemical Society: Washington, DC, 1996.
(3) Winnik, M. A.; Yelta, A. *Curr. Opin. Colloid Interface Sci.* **1997**, *2*, 424.
(4) Glass, J. E., Ed. *Associative Polymers in Aqueous Solution*; Advances in Chemistry 765; American Chemical Society, Washington, DC, 2000.
(5) Aubry, T.; Moan, M. *J. Rheol.* **1994**, *38*, 1681.
(6) Nyström, B.; Kjoniksen, A. L.; Iversen, C. *Adv. Colloid Interface Sci.* **1999**, *79*, 81.
(7) Jimerez Regalado, E.; Selb, J.; Candau, F. *Macromolecules,* **1999**, *32*, 8580.
(8) Candau, F.; Selb, J. *Adv. Colloid Interface Sci.* **1999**, *79*, 149.
(9) Rubinstein, M.; Dobrynin A. V. *Curr. Opin. Colloid Interface Sci.* **1999**, *4*, 83.
(10) Leibler, L.; Rubinstein, M.; Colby, R. H. *Macromolecules* **1991**, *24*, 4701.
(11) Rubinstein, M.; Semenov, A. N. *Macromolecules* **2001**, *34*, 1058.
(12) Caritey, J. P. These Universite de Rouen, France, 1994.
(13) Aubry, T.; Moan, M. *J. Rheol.* **1996**, *40*, 441.
(14) Chase, B.; Krauss, K.; Lantz, T.; Chmilowski, W. *Oilfield Rev.* **1997**, Autumn, 20.
(15) Sullivan P. F.; Huang, H.; Nelson, E. Presented at the 75th Annual Meeting, The Society of Rheology, Oct 2003; Paper SM43.
(16) Maitland, G. C. *Curr. Opin. Colloid Interface Sci.* **2000**, *5*, 301.
(17) Qu, Q.; Nelson, E.; Willberg, D.; Samuel, M.; Lee, J.; Chang, F.; Card, R.; Vinod, P.; Brown, J.; Thomas, R. U.S. Patent 6 435 277, 2002.
(18) Raghavan, S. R.; Kaler, E. *Langmuir* **2001**, *17*, 300.
(19) Croce, V.; Cosgrove, T.; Maitland, G.; Hughes, T.; Karlsson, G. *Langmuir* **2003**, *19*, 8536.
(20) Couillet, I.; Hughes, T.; Maitland, G.; Candau, F.; Candau S. J.; *Langmuir* **2004**, *20*, 9541.
(21) Goddard, E. D., Ananthapadmanabhan, K. P., Eds. *Interactions of surfactants with polymers and proteines*; CRC Press: Boca Raton, FL, 1993.
(22) Hansson, P.; Lindman, B. *Curr. Opin. Colloid Interface Sci.* **1996**, *1*, 604.
(23) Winnik, F. M.; Regismond, S. T. A. *Colloids Surf. A, Physicochem. Eng. Aspects* **1996**, *118*, 1.
(24) Kwak, J. C. T., Ed. *Polymers-Surfactants Systems*; Surfactant Science Series 77; Dekker: New York, 1998.
(25) Sau, A. C.; Landoll, L. M. In *Polymers in Aqueous Media: Performance through Association*; Glass, J. E., Ed.; Advances in Chemistry 223; American Chemical Society: Washington, DC, 1989; p 343.
(26) Tanaka, R.; Meadows, J.; Phillips, G. O.; Williams, P. A. *Carbohydr. Polym.* **1990**, *12*, 443.
(27) Iliopoulos, L.; Wang, T. K.; Audebert, R. *Langmuir* **1991**, *7*, 617.
(28) Biggs, S.; Selb, J.; Candau, F. *Langmuir* **1992**, *8*, 838.
(29) Chang, Y.; Lochhead, R. Y.; McCormick, C. L. *Macromolecules* **1994**, *27*, 2145.
(30) Nyström, B.; Thuresson, K.; Lindman, B. *Langmuir* **1995**, *11*, 1994.
(31) Xie, X.; Hogen-Esch, T. E. *Macromolecules* **1996**, *29*, 1734.
(32) Panmai, S.; Prudhomme, R. K.; Peiffer, D. G. *Colloids Surf. A.; Physicochem. Eng. Aspects* **1999**, *147*, 3.
(33) Piculell, L.; Guillemet, F.; Thuresson, K.; Shubin, V.; Ericsson, O. *Adv. Colloid Interface Sci.* **1996**, *63*, 1.
(34) Jimenez Regalado, E.; Selb, J.; Candau, F. *Langmuir* **2000**, *16*, 8611.
(35) Peiffer D. G.; *Polymer* **1990**, *31*, 2353.
(36) McCormick, C. L.; Nonaka, T.; Johnson, C. B. *Polymer* **1988**, *29*, 731.
(37) Zhang, Y. X.; Da, A. H.; Butler, G. B.; Hogen-Esch, T. E. *J. Polym. Sci., Polym. Chem. Ed.* **1992**, *30*, 1383.
(38) Hwang, F. S.; Hogen-Esch, T. E. *Macromolecules* **1995**, *28*, 3328.
(39) Biggs, S.; Selb, J.; Candau, F. *Polymer* **1993**, *34*, 580.
(40) Caputo, M. R.; Selb, J.; Candau, F. *Polymer* **2004**, *45*, 231.
(41) Volpert, E.; Selb, J.; Candau, F. *Polymer* **1998**, *39*, 1025.
(42) Berret, J. F.; Roux, D. C.; Porte, G. *J. Phys. II* **1994**, *4*, 1261.
(43) Grand, C.; Arrault, J.; Cates, M. E. *J. Phys. II* **1997**, *7*, 1071.
(44) Oda, R.; Narayanan, J.; Hassan, P. A.; Manohar, C.; Salkar, R. A.; Kern, F.; Candau, S. J. *Langmuir* **1998**, *14*, 4364.
(45) Klucker, R.; Candau, F.; Schosseler, F. *Macromolecules* **1995**, *28*, 6416.
(46) de Gennes, P. G. *Scaling Concepts in Polymer Physics*; Cornell University Press: London, 1979.
(47) Graessley, W. W. *Polymer* **1980**, *21*, 258.
(48) Colby, R. H.; Rubinstein, M.; Daoud, M. *J. Phys. II (Paris)* **1994**, *4*, 1299.
(49) Grosberg, A. Y.; Khokhlov, A. R. *Statistical Physics of Macromolecules*; A.I.P. Press: New York, 1994.
(50) Adam, M.; Lairez, D.; Raspaud, E.; *J. Phys. II* **1992**, *2*, 2067.
(51) Kavassalis, T. A.; Noolandi, J. *Phys. Rev. Lett.* **1987**, *59*, 2674.
(52) Granek, R. *Langmuir* **1994**, *10*, 1627.
(53) Annable, T.; Buscall, R.; Ettelaie, R.; Whittlestone, D. *J. Rheol.* **1993**, *37*, 695.
(54) Larson, R. G.; *The structure and rheology of complex fluids*, New York: Oxford University Press: Oxford, U.K., 1999.
(55) Schulz, D. N., Glass, J. E. Eds. *Polymers as Rheology Modifiers*, ACS Symposium Series 462; American Chemical Society: Washington, DC, 1991.
(56) Tam, K. C.; Jenkins, R. D.; Winnik, M. A.; Bassett, D, R. *Macromolecules* **1998**, *31*, 4149.
(57) Morris, E. R.; Cutler, A. N.; Ross-Murphy S. B.; Rees, D. A.; Price, J. *Carbohydr. Polym.* **1981**, *1*, 5.
(58) Doi, M.; Edwards, S. F. *The Theory of Polymer Dynamics*; Clarendon Press: Oxford, England, 1986.
(59) Cates, M. E. *Macromolecules* **1987**, *20*, 2289.
(60) Spenley, N. A.; Cates, M. E.; McLeish, T. C. B. *Phys. Rev. Lett.* **1993**, *71*, 939.
(61) English, R. B.; Laurer, J. H.; Spontak, R. J.; Khan, S. A. *Ind. Eng. Chem. Res.* **2002**, *41*, 6425.
(62) Rubinstein, M.; Semenov, A. N. *Macromolecules* **1998**, *31*, 1386.
(63) Lequeux, F. *Europhys. Lett.* **1992**, *19*, 675.

MA0501592